

The Use of Fluorescently Labeled ARC1779 Aptamer for Assessing the Effect of H₂O₂ on von Willebrand Factor Exocytosis

Piotr P. Avdonin¹, Sergey K. Trufanov¹, Elena Yu. Rybakova¹,
Aleksandra A. Tsitrina¹, Nikolay V. Goncharov^{2,3}, and Pavel V. Avdonin^{1,*}

¹*Koltsov Institute of Developmental Biology, Russian Academy of Sciences, 119334 Moscow, Russia*

²*Sechenov Institute of Evolutionary Physiology and Biochemistry, Russian Academy of Sciences, 194223 St. Petersburg, Russia*

³*Research Institute of Hygiene, Occupational Pathology and Human Ecology,
Federal Medical-Biological Agency, 188663 Kuzmolovsky, Leningrad Region, Russia*

^a*e-mail: pvavdonin@yandex.ru*

Received June 5, 2020

Revised October 15, 2020

Accepted October 15, 2020

Abstract—Here, we propose a new approach for quantitative estimation of von Willebrand factor (vWF) exposed on the surface of endothelial cells (ECs) using the ARC1779 aptamer that interacts with the vWF A1 domain. To visualize complex formation between vWF and the aptamer, the latter was conjugated with the Cy5 fluorescent label. Cultured human umbilical vein endothelial cells (HUVEC) were stained with the ARC1779-Cy5 conjugate and imaged with a fluorescence microscope. The images were analyzed with the CellProfiler software. vWF released from the Weibel–Palade bodies was observed as bright dot-like structures of round and irregular shape, the number of which increased several times after HUVEC exposure to histamine or thrombin. Staining with ARC1779-Cy5 also revealed long filamentous vWF structures on the surface of activated HUVEC. vWF secretion by ECs is activated by the second messengers cAMP and Ca²⁺. There is evidence that hydrogen peroxide also acts as a second messenger in ECs. In addition, exogenous H₂O₂ formed in leukocytes can enter ECs. The aim of our study was to determine the effect of H₂O₂ on the vWF exposure at the surface of HUVEC using the proposed method. It was shown that hydrogen peroxide at concentration 100 μM, which is lower than the cytotoxicity threshold of H₂O₂ for cultured HUVEC, increased several times the number of dot-like structures and total amount of vWF exposed on plasma membrane of HUVEC, which suggest that H₂O₂ acts as a mediator that activates exocytosis of Weibel–Palade bodies and vWF secretion in the vascular endothelium during inflammation and upon elevated generation of endogenous reactive oxygen species in ECs.

DOI: 10.1134/S0006297921020012

Keywords: von Willebrand factor, aptamers, hydrogen peroxide, endothelial cells, secretion

INTRODUCTION

More than a half of all pharmaceutical preparations are ligands of membrane receptors [1, 2]. The vast majority of these preparations are natural or artificially synthesized low molecular weight compounds. Most of them are not very selective – as a rule, they affect several targets in the cells. The design of exclusively specific therapeutics based on humanized antibodies is a new direction of pharmacology that has been intensively growing due to

the development of genetic engineering and molecular immunology techniques. Conjugates obtained by the attachment of various labels and toxins to the antibodies generated against receptors, components of complement system, and other proteins can be used simultaneously as diagnostic tools and therapeutic agents. This approach has been a basis for the new direction of biomedical studies – theranostics, in which antibodies are used as platforms for attaching markers for visualization of pathological features and components exerting the therapeutic effect [3].

The SELEX (systematic evolution of ligands by exponential enrichment) method was suggested in 1990 for designing aptamers – short single-stranded DNA or

Abbreviations: EC, endothelial cell; HUVEC, human umbilical cord vein endothelial cells; vWF, von Willebrand factor.

* To whom correspondence should be addressed.

RNA oligonucleotides with unique sequences exhibiting high affinity and specificity for the targets of various nature, such as cell surface proteins and polysaccharides, low-molecular-weight compounds, metal ions, etc. [4-7]. The affinity and the selectivity of aptamers are comparable to those of antibodies. A technique for selection of aptamers against different types of cells, including cancer cells was developed [8]. At present, several aptamers are tested in clinical trials for the treatment of oncological and blood disorders [9, 10]. Aptamers have a number of advantages in comparison to antibodies, such as structure reproducibility, high thermal stability, lesser immunogenicity, and possibility of long-term storage in a dry form [10]. It was demonstrated that aptamers can be as well used in histochemical studies [11] and flow cytometry [12] instead of antibodies.

One of the targets for antibodies and aptamers is the von Willebrand factor (vWF), which is a blood plasma glycoprotein secreted by endothelial cells (ECs) and involved in hemostasis. vWF is released into the blood by ECs as a population of giant multimeric molecules with a molecular mass up to 20,000 kDa, which are formed from ~250-kDa vWF monomers linked by disulfide bonds [13]. The vWF molecule contains regularly repeating structural A1 domain that mediates interactions of this factor with the glycoprotein 1b on the membranes of platelets. The binding of platelets to A1 domain in the unfolded vWF molecule initiates blood clot formation in damaged arterioles and capillaries in order to stop the bleeding. Excessive accumulation of vWF or its increased activity caused by mutations result in the microvascular thrombosis and development of thrombotic microangiopathies. Nano-antibody against the A1 domain caplacizumab is used for the treatment of thrombotic thrombocytopenic purpura [14]. Another A1-binding therapeutic agent is ARC1779 aptamer that was found to be effective in the treatment of type 2B von Willebrand disease [15-17]. An improved SELEX method that uses unnatural hydrophobic base for creating oligonucleotide libraries of random sequences (ExSELEX) was instrumental in the synthesis of a new, more efficient aptamer against vWF [18].

Antibodies are widely used in the studies of membrane receptors and intracellular proteins. Immunofluorescence staining is used for the evaluation of the expression levels of membrane and intracellular proteins and their location. One of the issues that requires more detailed studying is the mechanism involved in the regulation of vWF secretion in ECs. Anti-vWF antibodies can be used to estimate the vWF exposure on the plasma membrane. For this purpose, fixed ECs are incubated with the primary antibodies followed by incubation with the fluorescently labeled secondary antibodies [19]. In this work, we attempted to evaluate the vWF exocytosis using the ARC1779 aptamer conjugated with the fluorescent Cy5 dye. Currently, several aptamers have been

developed that bind to the vWF via its A1 domain, thus blocking its interaction with platelets [17, 18, 20, 21]; however, only ARC1779 has been approved for the therapeutic use so far. Using the ARC1779-Cy5 conjugate, we observed the opening of individual secretory vesicles on the EC surface and investigated the regulation of this process in live cells. We demonstrated that hydrogen peroxide at the concentrations that could be reached in blood vessels stimulate exocytosis of the Weibel-Palade bodies and promote exposure of vWF on the plasma membrane of ECs.

MATERIALS AND METHODS

Human umbilical vein endothelial cells (HUVEC) were isolated as described in [22] and cultured in M199 medium containing 20% fetal bovine serum (Sigma-Aldrich, USA) and endothelial growth supplement produced from frozen rabbit brains (Krolinfo Ltd., Novaya, Moscow Region, Russia) as described by Maciag et al. [23]. The cells were identified based on the morphological criteria and the presence of vWF, angiotensin-converting enzyme, and CD31, CD54, and CD61 surface proteins [24]. Isolated HUVEC were cultured in an atmosphere containing 5% CO₂ and used in the experiments after 2-4 passages; Accutase (Sigma-Aldrich) was used to detach the cells for passaging.

The ARC1779 aptamer (USA patent US20090203766A1; Archemix Corp., USA) with the 5'-conjugated Cy5 dye (Cy5-mGmCmGmUdGdCdAmGmUmGmCmCmUmUmCmGmGmCdCmG-s-dTmGdCdGdGdTmGmCdCmUdCdCmGmUdCmAmCmGmC, where *m* is 2'-OMe and *s* is phosphorothioate bond) was used for HUVEC staining. The scrambled Cy5-mGmGmCmCdAdGdCmCmUmCmUmCmCmUmGmGmUmGdGmG-s-TmCdGdCdCTmAmGdGmUdCdGmGmGdCmCmCmU oligonucleotide with the same nucleotide ratio as ARC1779 was used as a control. The oligonucleotides were synthesized by the DNK Sintez Company (Russia).

To evaluate the effects of histamine (100 μM), thrombin (1 U/ml), and hydrogen peroxide (100 μM) on the vWF exocytosis, HUVEC grown in a 24-well plate were washed from the growth medium with physiological saline solution (PSS, pH 7.4) containing 145 mM NaCl, 5 mM KCl, 10 mM HEPES, 1 mM MgCl₂, 1 mM CaCl₂, and 10 mM glucose. The cells were incubated in the presence or absence of the activator at 32-34°C for 20 min. Next, the medium was aspirated and 100 μl of ARC1779-Cy5 in the hybridization medium containing 0.1 mg/ml tRNA (Roche Diagnostics, Switzerland), 1 mg/ml bovine serum albumin (BSA; Amresco, USA), 5 mM MgCl₂, 25 mM glucose, 2.67 mM KCl, 1.47 mM KH₂PO₄, 136.9 mM NaCl, and 8.10 mM Na₂HPO₄ was added to each well followed by incubation for 20 min at 32°C. For

nucleus staining, 1 $\mu\text{g}/\text{ml}$ Hoechst 33342 (Thermo Fisher Scientific, USA) was added to the medium. ARC1779-Cy5 concentration in all experiments except concentration-dependence experiment was 50 nM. After incubation, the cells were washed twice with phosphate buffered saline (PBS, Thermo Fisher Scientific) to remove unbound ARC1779-Cy5 and 200 μl of FluoroBriteTM DMEM (Thermo Fisher Scientific) was added. The cells were immediately imaged with a Leica DMI 6000 fluorescence microscope equipped with an HCX PL FLUOTAR L 20.0 \times 0.40 DRY objective, diode light sources with the wavelengths of 385 and 620 nm, and A4 and TX2 filters (Leica, Germany). Fluorescence intensity, the number of vWF structures per cell were calculated following the processing of the mosaic images (1.5×2 mm) from the wells of 48-well plates were performed. The number of the cells in the 1.5×2 mm area was 2800-3000. The images were analyzed with the open-access CellProfiler program (<http://cellprofiler.org/releases>) [25] (detailed description of the application of this program for the analysis of images of ECs was published in [26]). The total number of analyzed frames was 96-128 (16 frames for each well in a 48-well plate). The data were obtained in three independent experiments using different HUVEC preparation. In each experiment there were at least six control and six test wells. The total number of vWF structures stained with ARC1779-Cy5 and exposed on the cell surface and the average brightness (fluorescence intensity per cell) were determined. The obtained data are presented in arbitrary units as mean \pm standard error of mean. The significance of differences was determined using the Student's *t*-test in the Excel program and the one-way ANOVA using the MedCalc program (MedCalc Software Ltd., Belgium).

For immunofluorescence staining, the cells were fixed with 4% paraformaldehyde in PBS for 20 min on ice and then washed carefully with PBS containing 1% BSA.

Primary antibodies against vWF (rabbit anti-human vWF, Dako, France; dilution 1 : 500; initial antibody concentration, 3.2 mg/ml) were applied in the same buffer followed by the overnight incubation at 4°C. Next, the cells were washed and incubated with a mixture of secondary antibodies (goat anti-rabbit AlexaFluor 488, Invitrogen, USA; dilution, 1 : 1000), wheat germ agglutinin AlexaFluor 488 (Invitrogen, dilution, 1 : 500), and 1 $\mu\text{g}/\text{ml}$ Hoechst 33258 nuclear dye (Sigma-Aldrich) for 1.5 h at room temperature. The cells were then washed with PBS containing 1% BSA, placed into saturated fructose solution, and analyzed with a Leica DMI 6000 fluorescence microscope (Leica). The parameters for image capture were adjusted for the brightest samples and remained the same in the course of the entire experiment. The mosaic image of the central part (1.5×2 mm) of each well consisting of 25 microscopic fields was acquired using the high-speed adaptive autofocus mode. For each sample, 25 images were captured (16 frames per image) in 3 fluorescent channels with the 8-bit color depth coding. The fluorescence intensity of stained vWF in each frame in control HUVEC and cells activated with H_2O_2 or thrombin was evaluated using the CellProfiler program.

RESULTS AND DISCUSSION

The images of HUVEC stained with ARC1779-Cy5 (50 nM) are shown in Fig. 1a. Prior to the aptamer addition, the cells were incubated for 20 min with histamine (vWF secretion activator). Cell nuclei were stained with Hoechst 33342. ARC1779-Cy5 stained small structures with predominantly round or irregular shape. To evaluate the specificity of the vWF staining with ARC1779-Cy5, a conjugate of Cy5 with scrambled oligonucleotide of the same length and nucleotide ratio was used as a negative control (Fig. 1b). The control oligonucleotide did not

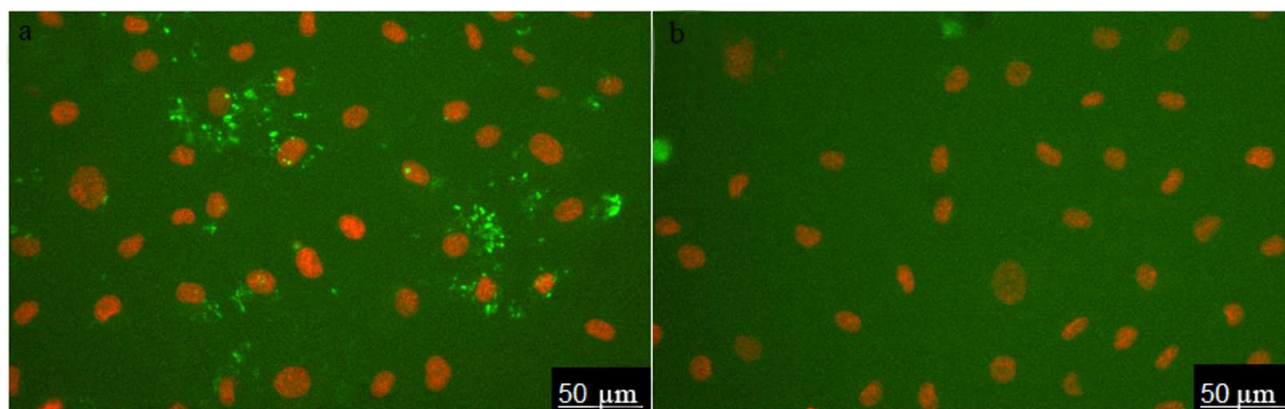


Fig. 1. HUVEC activated with histamine (100 μM) and stained with 50 nM ARC1779-Cy5 (a) and 50 nM Cy5-labeled control oligonucleotide (b). (Color versions of Figs. 1-5 are available in the online version of this article and can be accessed at <https://www.springer.com/journal/10541>).

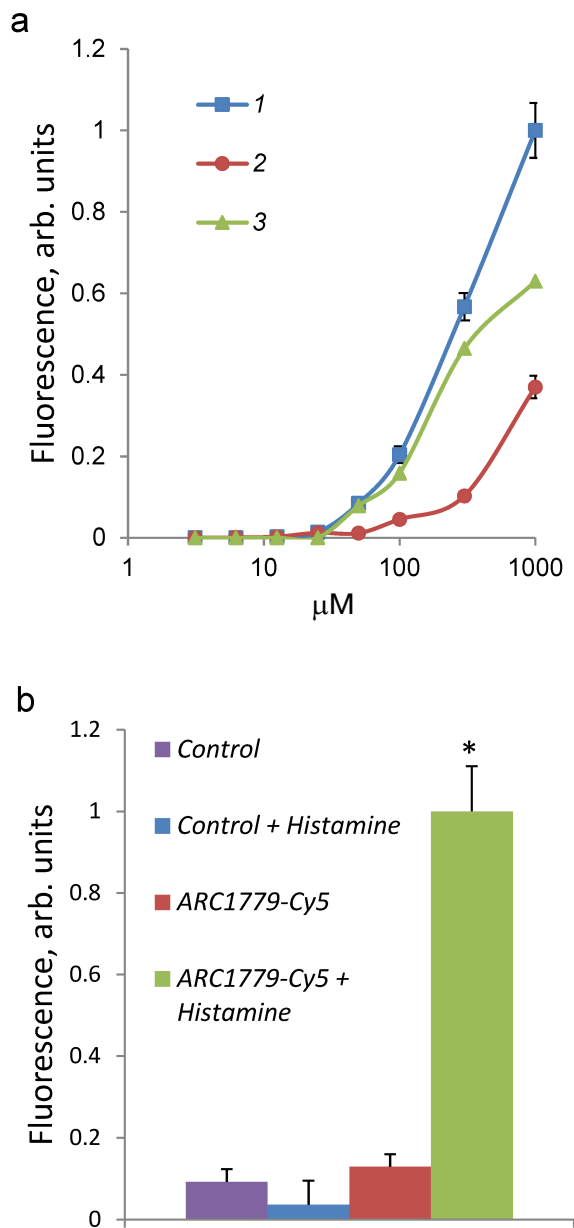


Fig. 2. a) Dependence of HUVEC fluorescence intensity on the concentration of ARC1779-Cy5 (curve 1) or control oligonucleotide (curve 2). Curve 3 represents the difference between curve 1 (total binding) and curve 2 (non-specific binding) and corresponds to the specific ARC1779-Cy5 interaction with the vWF. b) Fluorescence intensity of HUVEC stained with 50 nM ARC1779-Cy5 (ARC1779-Cy5, ARC1779-Cy5 + Histamine) or 50 nM control oligonucleotide (Control, Control + Histamine) in the absence or presence of 100 μM histamine; * $p < 0.01$ significant differences between ARC1779-Cy5 + Histamine and ARC1779-Cy5 or control with or without histamine.

bind to the live cells; large bright spots in Fig. 1b are stained nucleus-free fragments of dead cells.

The dependence of the ARC1779-Cy5 binding to HUVEC on the aptamer concentration (3.1 nM–1 μM) is presented in Fig. 2. The total brightness of the stained

vWF structures on the cell surface was calculated with the CellProfiler program. The ARC1779-Cy5 staining of vWF on the cell membrane was observed at the aptamer concentration of 50 nM and higher (Fig. 2a, curve 1). The brightness of the staining increased with the ARC1779-Cy5 concentration increase to 1 μM. The non-specific binding of the label was determined using corresponding concentrations of the labeled control oligonucleotide, which did not stain the cells at the concentrations up to 100 nM. Further elevation of its concentration resulted in the fluorescence intensity increase due to non-specific binding (Fig. 2a, curve 2). Curve 3 in Fig. 2a represents the difference between the fluorescence intensities of ARC1779-Cy5 and control oligonucleotide and corresponds to the specific interaction of ARC1779-Cy5 with the vWF. The EC_{50} value for the ARC1779-Cy5 binding to VWF was 287 nM (95% confidence interval from 155 to 589 nM). In further experiments, we used 50 nM ARC1779-Cy5, as the non-specific binding at this concentration was low. The relative fluorescence intensities of the non-activated and histamine-activated HUVEC after the staining with 50 nM ARC1779-Cy5 or 50 nM control oligonucleotide are shown in Fig. 2b. It can be seen that histamine did not affect the non-specific oligonucleotide binding with the cells. In the absence of histamine, the fluorescence was only slightly above the background, which indicates low levels of vWF exposure on the HUVEC plasma membrane in the absence of activators.

Next, we use the above-described experimental approach to study the regulation of vWF exocytosis. vWF exocytosis in ECs is stimulated by endocrine factors, including thrombin [27], vasopressin [28], histamine [29], serotonin [30], adrenalin [31], purine nucleotides [32], cytokines, and growth factors [33, 34]. Their action is mediated by the second messengers cAMP and Ca^{2+} [35]. It is known that hydrogen peroxide also serves as a second messenger in ECs [36]. Moreover, EC functioning is affected by the exogenous H_2O_2 secreted by neutrophils. We have shown previously that exogenously added H_2O_2 penetrates into ECs [26]. H_2O_2 acts as a second messenger by inhibiting protein tyrosine phosphatases [37]. In ECs, H_2O_2 selectively promotes the effect of agonists of 5-HT1B and 5-HT2B receptors [38] and stimulates two-pore endolysosomal calcium channels [39]. The data on the effect of H_2O_2 on vWF secretion are quite contradictory. It was shown previously that exogenous superoxide anion increases vWF secretion by cultured ECs; however, no reliable effect of H_2O_2 added to the medium at the concentrations up to 0.5 mM was observed [40]. On the contrary, Yang et al. [41] reported a 1.5–2-fold increase in the vWF secretion after stimulation with 0.5 mM H_2O_2 . In any case, the effect of cytotoxic H_2O_2 concentrations has been established. We have previously shown using immunocytofluorimetry and enzyme-linked immunoassay that hydrogen peroxide at the con-

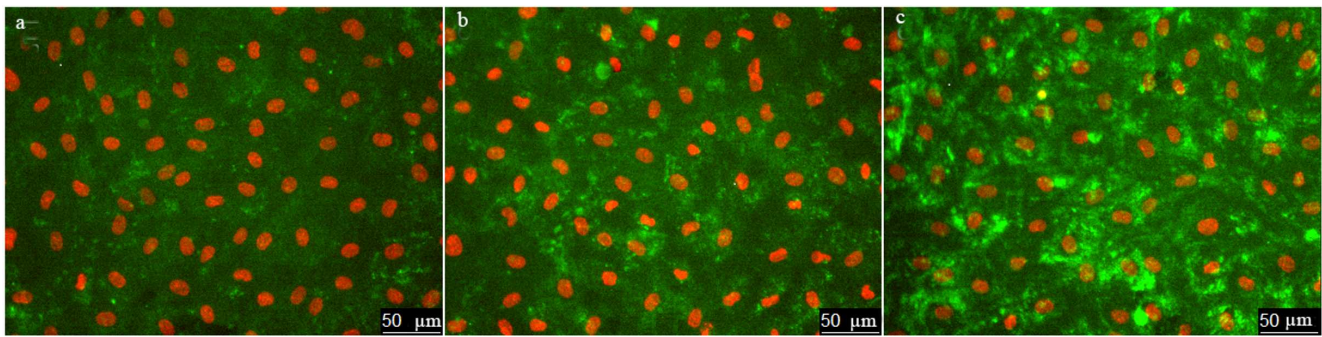


Fig. 3. Effect of H_2O_2 and thrombin on vWF exocytosis in HUVEC. Cell nuclei stained with Hoechst 33342 and vWF stained with ARC1779-Cy5 are shown in control cells (a) and after treatment with $100 \mu M H_2O_2$ (b) or 1 U/ml thrombin (c). ARC1779-Cy5 concentration, $50 nM$.

centration of $100 \mu M$ which is below the cytotoxicity level for the cultured HUVEC caused an increase in the amount of vWF exposed on the cell surface and activated vWF secretion into the extracellular medium [26]. In this work, we continued these studies using the new approach that employed the ARC1779 aptamer conjugated with the fluorescent Cy5 label. Unlike traditional immunofluorescent staining, HUVEC staining with ARC1779-Cy5 was performed in live cells. It was demonstrated that 20 min after addition of $100 \mu M H_2O_2$, the number of cells stained with ARC1779-Cy5 drastically increased (Fig. 3b) in comparison with the control (Fig. 3a). The average fluorescence intensity (Fig. 4a) increased 4.47-fold ($p < 0.01$). The average number of stained dot-like vWF structures per cell was 5.79 after H_2O_2 addition, which was 4.3 times higher than the number of stained vWF structures in the control (Fig. 4b). The extent of the H_2O_2 -induced increase in the number of vWF-positive structures actually coincides with the extent of the fluorescence increase. It follows from this that the increase in the vWF content on the HUVEC surface after the treatment with H_2O_2 occurred predominately due to the increase in the number of opened secretory vesicles – Weibel–Palade bodies. It was shown previously [19, 42] using correlative immunofluorescence and electron microscopy image analysis that vWF secretion is accompanied by the coalescence of Weibel–Palade bodies with the formation of larger secretory capsules. The capsules open on the plasma membrane creating pores from 0.5 to several μm in diameter. The size of the observed dot-like vWF structures was within this range as well; the average maximum and minimum Feret diameters were 0.97 and $0.45 \mu m$, respectively, in the control cells and 1.02 and $0.48 \mu m$, respectively, in the H_2O_2 -treated cells.

Immunocytofluorimetry detected only a 2-fold increase in the content of vWF exposed on the cell surface after H_2O_2 treatment [26]. We believe that the reason why this effect was more pronounced in the case of ARC1779-Cy5 staining is omission of the fixation step, which

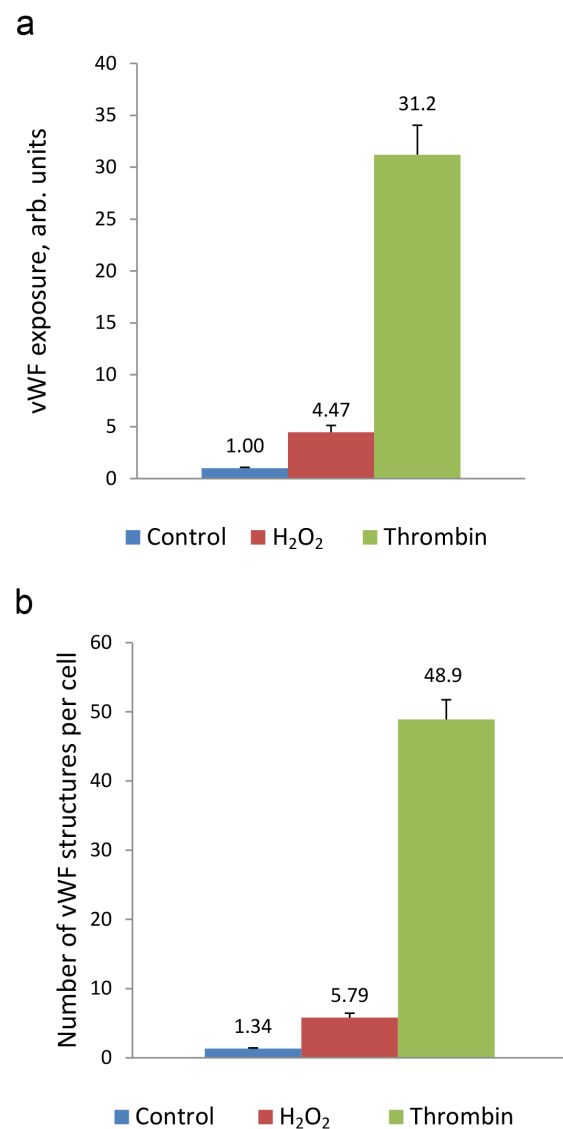


Fig. 4. ARC1779-Cy5 staining of the vWF exposed on the surface of HUVEC (a) and average number of dot-like vWF structures in a single cell (b) in control cells and cells treated with $100 \mu M H_2O_2$ or 1 U/ml thrombin.

could cause additional fusion of the secreted vesicles with the membrane. Comparison of the data presented in Figs. 2b and 4a revealed that the effect of H_2O_2 on the vWF exposure was comparable with the effect of 100 μM histamine. Thrombin, which was used as a positive control, exerted a much more pronounced effect, as it increased the vWF exposure on the plasma membrane 31.2-fold (Fig. 4a), while the number of exposed vWF structures per number of nuclei (i.e., per single cell) increased 36.5-fold (Fig. 4b). The fact that these values are close indicates that, similarly to H_2O_2 , thrombin increased the vWF exposure due to the increase in the number of opened secretory vesicles. In addition to the dot-like structures, one can see individual stained filaments tens of microns in length, which are formed by ultra-large vWF multimers (Fig. 3c).

Immunocytofluorescence technique is a standard approach for the evaluation of vWF exposure on the sur-

face of ECs. In this study, instead of antibodies, we used a conjugate of the ARC1779 aptamer with the Cy5 fluorescent dye to stain vWF, as this method allows staining of live cells (vs. fixed cells in the immunocytofluorescence technique). We also compared the results of ARC1779-Cy5 with the results produced with the immunocytofluorescence technique. The images of the control cells and cells treated with H_2O_2 or thrombin stained with the anti-vWF antibodies are shown in Fig. 5. The final concentration of primary anti-vWF antibodies was 40 nM (1 : 500 dilution of the initial IgG preparation with the concentration 3.2 mg/ml or 20 μM). The same cell batch incubated under the same conditions was used for vWF staining with ARC1779-Cy5 (Fig. 3). The images acquired after antibody staining (Fig. 5, a-c) were similar to those produced using ARC1779-Cy5 (Fig. 3). The sharpness of the images was higher in the case of antibodies, because the second antibodies produced more intense staining

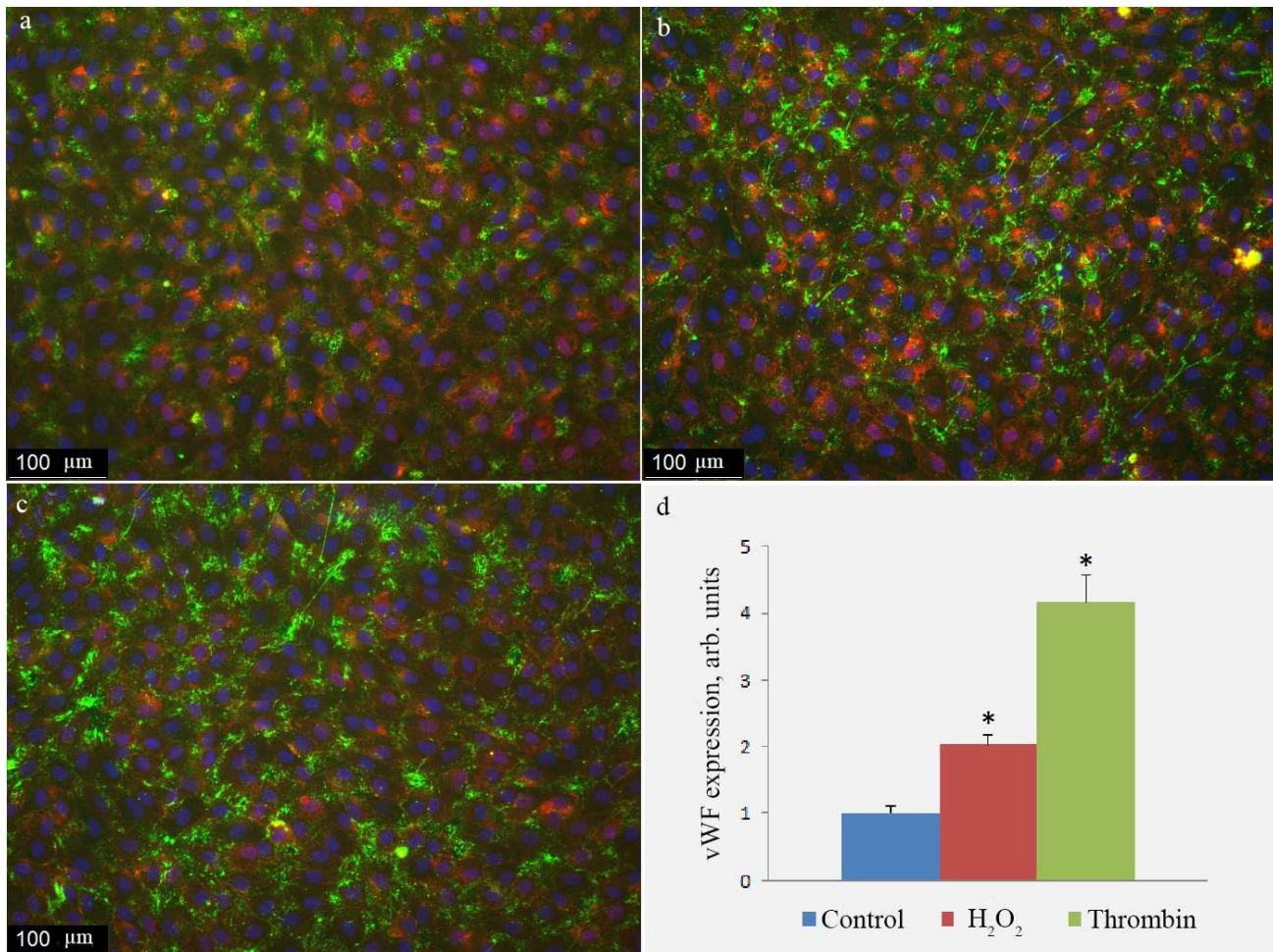


Fig. 5. Antibody staining of vWF on the surface of HUVEC in control cells (a) and cells treated with 100 μM H_2O_2 (b) or 1 unit/ml thrombin (c). vWF exposure on the cell surface determined with the immunofluorescence technique in control cells and cells activated by H_2O_2 or thrombin (d); (*) significant differences from the control at $p < 0.01$. To visualize cell boundaries, the cells were stained with the WGA AlexaFluor 594 conjugate. The image is presented in pseudocolors: green, vWF; blue, nuclei; purple, lectin.

relative to the background than ARC1779-Cy5. However, the fluorescence of the antibody-stained vWF after incubation with H₂O₂ or thrombin increased only 2- and 4-fold, respectively, vs. the control (Fig. 5c), while in the experiments with ARC1779-Cy5, the increase was 4.5- and 31-fold, respectively (Fig. 4a). The staining of the histamine-activated cells with the antibodies produced less effect than staining with the aptamer (data not shown). As was mentioned above, we believe that the less pronounced effect of agonists on the vWF surface exposure observed in the immunofluorescence staining could be explained by the artefact involving additional exocytosis of secretory granules during fixation. Hence, the use of ARC1779-Cy5 produces more credible picture of vWF exocytosis than the use of antibodies, despite the reduced contrast of the image obtained with ARC1779-Cy5.

We assume that the ratio of between the intensity of specific vWF staining and background could be improved by using aptamers that have been developed after ARC1779 and currently undergo clinical trials for the treatment of thrombotic microangiopathy. Thus, it was found that the TAGX-0004 aptamer with one unnatural base in its nucleotide sequence suppresses platelet aggregation more efficiently than ARC1779 [17]. The pegylated aptamer BT200 suppresses vWF activity in the plasma with the IC₅₀ of 70 nM [43]. The efficacy of these two aptamers was determined in the platelet aggregation assay. Platelets also secrete vWF and expose it on the cell surface; hence ARC1779-Cy5 could be used for assessing their activation by the flow cytometry technique.

Here, we demonstrated clearly pronounced H₂O₂-induced activation of vWF exocytosis using ARC1779-Cy5. *In vivo*, hydrogen peroxide is produced endogenously by ECs [36], as well as released by neutrophils adhered on the surface of activated endothelium [44]. According to the calculations reported by Jones [45], the rate of H₂O₂ formation in an organism can reach up to 500 μmol/kg/min. The results of the H₂O₂ concentration assessment under stationary conditions in the whole blood and in human and rat blood plasma obtained in different laboratories vary within a broad range – from several to tens of micromoles per liter of plasma and to hundreds of micromoles per liter of blood [46, 47]. The latter is due to the high concentration of H₂O₂ in erythrocytes and in neutrophils, even considering the difference in the content of these cells in the blood. Local concentration of H₂O₂ in the vicinity of endothelium could be significantly higher than the average concentration in the blood plasma. No noticeable toxic effect of H₂O₂ at the concentrations up to 150 μM was found in cultured HUVEC [48, 49]. Hence, the concentration of 100 μM used in our experiments was not toxic to the cultured HUVEC and corresponded to physiological conditions. It was shown previously that 5-100 μM H₂O₂ induces surface exposure of the major histocompatibility complex MHC1 and cell

adhesion molecule ICAM-1 in ECs [50]. These data provide additional information on the effect of H₂O₂ on the processes of secretion in ECs.

The obtained data are in agreement with the concept on the H₂O₂ role as a second messenger that regulates vWF exocytosis in ECs together with cAMP and Ca²⁺. In this regard, a question arises as to the effect of which neuroendocrine factors on the secretion of vWF in EC is mediated by H₂O₂. There are no direct data indicating participation of H₂O₂ in the receptor-dependent regulation of vWF exocytosis; however, there are indirect indications in the literature that corroborate this hypothesis. It is known that the VEGF receptors interact with the NADPH oxidase NOX4, and the same receptors (VEGFR2) mediate activation of the vWF secretion [51]. The proinflammatory cytokines IL-6, IL-9, and TNFα initiate vWF exocytosis [34], as well as formation of reactive oxygen species, including H₂O₂ [52]. However, in all these cases, no possible association between the stimulation of vWF secretion and H₂O₂ formation has been investigated. We demonstrated recently that the blocker of NADPH oxidases VAS2870 suppressed the vWF secretion induced by histamine [53]. Hence, further studies are required to elucidate the role of H₂O₂ in the transduction of agonist signals to the VWF metabolism. We believe that the developed method for the vital staining of vWF exposed on the surface of ECs could facilitate the progress in this area of research.

Funding. This work was supported by the Russian Science Foundation (project no. 18-15-00417) and the State Budget (no. 0088-2021-0008). Equipment was provided by the Center for Collective Use, Koltsov Institute of Developmental Biology, Russian Academy of Sciences.

Ethics declaration. The authors declare no conflict of interest. All procedures involving human participants were performed in accordance with the ethical standards of the institutional and/or national research committees and with the 1964 Helsinki declaration and its later amendments or comparable ethical standards.

Open access. This article is distributed under the terms of the Creative Commons Attribution 4.0 International License (<http://creativecommons.org/licenses/by/4.0/>), which permits unrestricted use, distribution, and reproduction in any medium, provided you give appropriate credit to the original author(s) and the source, provide a link to the Creative Commons license, and indicate if changes were made.

REFERENCES

1. Langmead, C. J., and Summers, R. J. (2018) Molecular pharmacology of GPCRs, *Br. J. Pharmacol.*, **175**, 4005-4008, doi: 10.1111/bph.14474.

2. Sriram, K., and Insel, P. A. (2018) G protein-coupled receptors as targets for approved drugs: how many targets and how many drugs? *Mol. Pharmacol.*, **93**, 251-258, doi: 10.1124/mol.117.111062.
3. Deyev, S. M., and Lebedenko, E. N. (2015) Supramolecular agents for theranostics, *Russ. J. Bioorg. Khim.*, **41**, 481-493, doi: 10.1134/s1068162015050052.
4. Ellington, A. D., and Szostak, J. W. (1990) *In vitro* selection of RNA molecules that bind specific ligands, *Nature*, **346**, 818-822, doi: 10.1038/346818a0.
5. Tuerk, C., and Gold, L. (1990) Systematic evolution of ligands by exponential enrichment: RNA ligands to bacteriophage T4 DNA polymerase, *Science*, **249**, 505-510, doi: 10.1126/science.2200121.
6. Wang, J., and Li, G. (2011) Aptamers against cell surface receptors: selection, modification and application, *Curr. Med. Chem.*, **18**, 4107-4116, doi: 10.2174/092986711797189628.
7. Spiridonova, V. A., Novikova, T. M., Sizov, V. A., Shashkovskaya, V. S., Titaeva, E. V., Dobrovolsky, A. B., Zharikova, E. B., and Mazurov, A. V. (2019) DNA aptamers to thrombin exosite I. Structure-function relationships and antithrombotic effects, *Biochemistry (Moscow)*, **84**, 1521-1528, doi: 10.1134/S0006297919120113.
8. Rahimizadeh, K., Al Shamaileh, H., Fratini, M., Chakravarthy, M., Stephen, M., Shigdar, S., and Veedu, R. N. (2017) Development of cell-specific aptamers: recent advances and insight into the selection procedures, *Molecules*, **22**, 2070, doi: 10.3390/molecules22122070.
9. Zhuo, Z., Yu, Y., Wang, M., Li, J., Zhang, Z., et al. (2017) Recent advances in SELEX technology and aptamer applications in biomedicine, *Int. J. Mol. Sci.*, **18**, 2142, doi: 10.3390/ijms18102142.
10. Zhang, Y., Lai, B. S., and Juhas, M. (2019) Recent advances in aptamer discovery and applications, *Molecules*, **24**, 941, doi: 10.3390/molecules24050941.
11. Bauer, M., Macdonald, J., Henri, J., Duan, W., and Shigdar, S. (2016) The application of aptamers for immunohistochemistry, *Nucleic Acid Ther.*, **26**, 120-126, doi: 10.1089/nat.2015.0569.
12. Zhang, P., Zhao, N., Zeng, Z., Feng, Y., Tung, C. H., Chang, C. C., and Zu, Y. (2009) Using an RNA aptamer probe for flow cytometry detection of CD30-expressing lymphoma cells, *Lab. Invest.*, **89**, 1423-1432, doi: 10.1038/labinvest.2009.113.
13. Sadler, J. E. (1998) Biochemistry and genetics of von Willebrand factor, *Annu. Rev. Biochem.*, **67**, 395-424, doi: 10.1146/annurev.biochem.67.1.395.
14. Duggan, S. (2018) Caplacizumab: first global approval, *Drugs*, **78**, 1639-1642, doi: 10.1007/s40265-018-0989-0.
15. Bae, O. N. (2012) Targeting von Willebrand factor as a novel anti-platelet therapy; application of ARC1779, an anti-vWF aptamer, against thrombotic risk, *Arch. Pharm. Res.*, **35**, 1693-1699, doi: 10.1007/s12272-012-1000-3.
16. Jilma-Stohlawetz, P., Knobl, P., Gilbert, J. C., and Jilma, B. (2012) The anti-von Willebrand factor aptamer ARC1779 increases von Willebrand factor levels and platelet counts in patients with type 2B von Willebrand disease, *Thromb. Haemost.*, **108**, 284-290, doi: 10.1160/TH11-12-0889.
17. Sakai, K., Someya, T., Harada, K., Yagi, H., Matsui, T., and Matsumoto, M. (2019) Novel aptamer to von Willebrand factor A1 domain (TAGX-0004) shows total inhibition of thrombus formation superior to ARC1779 and comparable to caplacizumab, *Haematologica*, **105**, 2631-2638, doi: 10.3324/haematol.2019.235549.
18. Matsunaga, K. I., Kimoto, M., and Hirao, I. (2017) High-Affinity DNA aptamer generation targeting von Willebrand factor A1-domain by genetic alphabet expansion for systematic evolution of ligands by exponential enrichment using two types of libraries composed of five different bases, *J. Am. Chem. Soc.*, **139**, 324-334, doi: 10.1021/jacs.6b10767.
19. Valentijn, K. M., van Driel, L. F., Mourik, M. J., Hendriks, G. J., Arends, T. J., Koster, A. J., and Valentijn, J. A. (2010) Multigranular exocytosis of Weibel-Palade bodies in vascular endothelial cells, *Blood*, **116**, 1807-1816, doi: 10.1182/blood-2010-03-274209.
20. Kovacevic, K. D., Buchtele, N., Schoergenhofer, C., Derhaschnig, U., Gelbenegger, G., Brostjan, C., Zhu, S., Gilbert, J. C., and Jilma, B. (2020) The aptamer BT200 effectively inhibits von Willebrand factor (VWF) dependent platelet function after stimulated VWF release by desmopressin or endotoxin, *Sci. Rep.*, **10**, 11180, doi: 10.1038/s41598-020-68125-9.
21. Nimjee, S. M., Dornbos, D., 3rd, Pitoc, G. A., Wheeler, D. G., Layzer, J. M., et al. (2019) Preclinical development of a vWF aptamer to limit thrombosis and engender arterial recanalization of occluded vessels, *Mol. Ther.*, **27**, 1228-1241, doi: 10.1016/j.ymthe.2019.03.016.
22. Goncharov, N. V., Sakharov, I., Danilov, S. M., and Sakandelidze, O. G. (1987) Use of collagenase from the hepatopancreas of the Kamchatka crab for isolating and culturing endothelial cells of the large vessels in man, *Bull. Eksp. Biol. Med.*, **104**, 376-378.
23. Maciag, T., Cerundolo, J., Ilsley, S., Kelley, P. R., and Forand, R. (1979) An endothelial cell growth factor from bovine hypothalamus: identification and partial characterization, *Proc. Natl. Acad. Sci. USA*, **76**, 5674-5678, doi: 10.1073/pnas.76.11.5674.
24. Kudryavtsev, I. V., Garnyuk, V. V., Nadeev, A. D., and Goncharov, N. V. (2014) Hydrogen peroxide modulates expression of surface antigens by human umbilical vein endothelial cells *in vitro*, *Biochemistry (Moscow) Supp. Ser. A Membr. Cell Biol.*, **8**, 97-102, doi: 10.1134/S1990747813050103.
25. Bray, M. A., Vokes, M. S., and Carpenter, A. E. (2015) Using CellProfiler for automatic identification and measurement of biological objects in images, *Curr. Protoc. Mol. Biol.*, **109**, 1-18, doi: 10.1002/0471142727.mb1417s109.
26. Avdonin, P. V., Tsitrina, A. A., Mironova, G. Y., Avdonin, P. P., Zharkikh, I. L., Nadeev, A. D., and Goncharov, N. V. (2017) Hydrogen peroxide stimulates exocytosis of von Willebrand factor in human umbilical vein endothelial cells, *Biol. Bull.*, **44**, 531-537, doi: 10.1134/s106235901705003x.
27. Hattori, R., Hamilton, K. K., Fugate, R. D., McEver, R. P., and Sims, P. J. (1989) Stimulated secretion of endothelial von Willebrand factor is accompanied by rapid redistribution to the cell surface of the intracellular granule membrane protein GMP-140, *J. Biol. Chem.*, **264**, 7768-7771.
28. Kaufmann, J. E., Oksche, A., Wollheim, C. B., Gunther, G., Rosenthal, W., and Vischer, U. M. (2000) Vasopressin-induced von Willebrand factor secretion from endothelial cells involves V2 receptors and cAMP, *J. Clin. Invest.*, **106**, 107-116, doi: 10.1172/JCI9516.

29. Esposito, B., Gambarà, G., Lewis, A. M., Palombi, F., D'Alessio, A., et al. (2011) NAADP links histamine H1 receptors to secretion of von Willebrand factor in human endothelial cells, *Blood*, **117**, 4968-4977, doi: 10.1182/blood-2010-02-266338.
30. Schluter, T., and Bohnensack, R. (1999) Serotonin-induced secretion of von Willebrand factor from human umbilical vein endothelial cells via the cyclic AMP-signaling systems independent of increased cytoplasmic calcium concentration, *Biochem. Pharmacol.*, **57**, 1191-1197.
31. Vischer, U. M., and Wollheim, C. B. (1997) Epinephrine induces von Willebrand factor release from cultured endothelial cells: involvement of cyclic AMP-dependent signalling in exocytosis, *Thromb. Haemost.*, **77**, 1182-1188.
32. Vischer, U. M., and Wollheim, C. B. (1998) Purine nucleotides induce regulated secretion of von Willebrand factor: involvement of cytosolic Ca²⁺ and cyclic adenosine monophosphate-dependent signaling in endothelial exocytosis, *Blood*, **91**, 118-127.
33. Matsushita, K., Yamakuchi, M., Morrell, C. N., Ozaki, M., O'Rourke, B., Irani, K., and Lowenstein, C. J. (2005) Vascular endothelial growth factor regulation of Weibel-Palade-body exocytosis, *Blood*, **105**, 207-214, doi: 10.1182/blood-2004-04-1519.
34. Bernardo, A., Ball, C., Nolasco, L., Moake, J. F., and Dong, J. F. (2004) Effects of inflammatory cytokines on the release and cleavage of the endothelial cell-derived ultralarge von Willebrand factor multimers under flow, *Blood*, **104**, 100-106, doi: 10.1182/blood-2004-01-0107.
35. Vischer, U. M. (2006) Von Willebrand factor, endothelial dysfunction, and cardiovascular disease, *J. Thromb. Haemost.*, **4**, 1186-1193, doi: 10.1111/j.1538-7836.2006.01949.x.
36. Breton-Romero, R., and Lamas, S. (2014) Hydrogen peroxide signaling in vascular endothelial cells, *Redox Biol.*, **2**, 529-534, doi: 10.1016/j.redox.2014.02.005.
37. Rhee, S. G., Kang, S. W., Jeong, W., Chang, T. S., Yang, K. S., and Woo, H. A. (2005) Intracellular messenger function of hydrogen peroxide and its regulation by peroxiredoxins, *Curr. Opin. Cell Biol.*, **17**, 183-189, doi: 10.1016/j.ceb.2005.02.004.
38. Avdonin, P. V., Nadeev, A. D., Mironova, G. Y., Zharkikh, I. L., Avdonin, P. P., and Goncharov, N. V. (2019) Enhancement by hydrogen peroxide of calcium signals in endothelial cells induced by 5-HT1B and 5-HT2B receptor agonists, *Oxid. Med. Cell. Longev.*, **2019**, 1701478, doi: 10.1155/2019/1701478.
39. Avdonin, P. V., Nadeev, A. D., Tsitritin, E. B., Tsitritina, A. A., Avdonin, P. P., Mironova, G. Y., Zharkikh, I. L., and Goncharov, N. V. (2017) Involvement of two-pore channels in hydrogen peroxide-induced increase in the level of calcium ions in the cytoplasm of human umbilical vein endothelial cells, *Dokl. Biochem. Biophys.*, **474**, 209-212, doi: 10.1134/S1607672917030152.
40. Vischer, U. M., Jornot, L., Wollheim, C. B., and Theler, J. M. (1995) Reactive oxygen intermediates induce regulated secretion of von Willebrand factor from cultured human vascular endothelial cells, *Blood*, **85**, 3164-3172.
41. Yang, S., Zheng, Y., and Hou, X. (2019) Lipoxin A4 restores oxidative stress-induced vascular endothelial cell injury and thrombosis-related factor expression by its receptor-mediated activation of Nrf2-HO-1 axis, *Cell. Signal.*, **60**, 146-153, doi: 10.1016/j.cellsig.2019.05.002.
42. Mourik, M. J., Valentijn, J. A., Voorberg, J., Koster, A. J., Valentijn, K. M., and Eikenboom, J. (2013) Von Willebrand factor remodeling during exocytosis from vascular endothelial cells, *J. Thromb. Haemost.*, **11**, 2009-2019, doi: 10.1111/jth.12401.
43. Zhu, S., Gilbert, J. C., Hatala, P., Harvey, W., Liang, Z., Gao, S., Kang, D., and Jilma, B. (2020) The development and characterization of a long acting anti-thrombotic von Willebrand factor (VWF) aptamer, *J. Thromb. Haemost.*, **18**, 1113-1123, doi: 10.1111/jth.14755.
44. Shappell, S. B., Toman, C., Anderson, D. C., Taylor, A. A., Entman, M. L., and Smith, C. W. (1990) Mac-1 (CD11b/CD18) mediates adherence-dependent hydrogen peroxide production by human and canine neutrophils, *J. Immunol.*, **144**, 2702-2711.
45. Jones, D. P. (2008) Radical-free biology of oxidative stress, *Am. J. Physiol. Cell. Physiol.*, **295**, C849-C868, doi: 10.1152/ajpcell.00283.2008.
46. Forman, H. J., Bernardo, A., and Davies, K. J. (2016) What is the concentration of hydrogen peroxide in blood and plasma? *Arch. Biochem. Biophys.*, **603**, 48-53, doi: 10.1016/j.abb.2016.05.005.
47. Varma, S. D., and Devamanoharan, P. S. (1991) Hydrogen peroxide in human blood, *Free Radic. Res. Commun.*, **14**, 125-131, doi: 10.3109/10715769109094124.
48. Nadeev, A. D., Kudryavtsev, I. V., Serebriakova, M. K., Avdonin, P. V., Zinchenko, V. P., and Goncharov, N. V. (2016) Dual proapoptotic and pronecrotic effect of hydrogen peroxide on human umbilical vein endothelial cells, *Cell Tiss. Biol.*, **10**, 145-151, doi: 10.1134/S1990519X16020097.
49. Yang, D., Liu, X., Liu, M., Chi, H., Liu, J., and Han, H. (2015) Protective effects of quercetin and taraxasterol against H₂O₂-induced human umbilical vein endothelial cell injury *in vitro*, *Exp. Ther. Med.*, **10**, 1253-1260, doi: 10.3892/etm.2015.2713.
50. Bradley, J. R., Johnson, D. R., and Pober, J. S. (1993) Endothelial activation by hydrogen peroxide. Selective increases of intercellular adhesion molecule-1 and major histocompatibility complex class I, *Am. J. Pathol.*, **142**, 1598-1609.
51. Xiong, Y., Huo, Y., Chen, C., Zeng, H., Lu, X., et al. (2009) Vascular endothelial growth factor (VEGF) receptor-2 tyrosine 1175 signaling controls VEGF-induced von Willebrand factor release from endothelial cells via phospholipase C-gamma 1- and protein kinase A-dependent pathways, *J. Biol. Chem.*, **284**, 23217-23224, doi: 10.1074/jbc.M109.019679.
52. Mo, S. J., Son, E. W., Rhee, D. K., and Pyo, S. (2003) Modulation of TNF-alpha-induced ICAM-1 expression, NO and H₂O₂ production by alginate, allicin and ascorbic acid in human endothelial cells, *Arch. Pharm. Res.*, **26**, 244-251.
53. Avdonin, P. V., Rybakova, E. Y., Avdonin, P. P., Trufanov, S. K., Mironova, G. Y., Tsitritina, A. A., and Goncharov, N. V. (2019) VAS2870 Inhibits histamine-induced calcium signaling and vWF secretion in human umbilical vein endothelial cells, *Cells*, **8**, 196, doi: 10.3390/cells8020196.